Published in final edited form as:
Proteins. 2009 May 15; 75(3): 628–637. doi:10.1002/prot.22274.

Structure of the S1S2 Glutamate Binding Domain of GluR3

Ahmed H. Ahmed, **Qi Wang**, **Holger Sondermann**, and **Robert E. Oswald**
Department of Molecular Medicine, Cornell University, Ithaca, NY 14853 USA

Abstract

Glutamate receptors are the most prevalent excitatory neurotransmitter receptors in the vertebrate central nervous system. Determining the structural differences between the binding sites of different subtypes is crucial to our understanding of neuronal circuits and to the development of subtype specific drugs. The structures of the binding domain (S1S2) of the GluR3 (flip) AMPA receptor subunit bound to glutamate and AMPA and the GluR2 (flop) subunit bound to glutamate were determined by X-ray crystallography to 1.9, 2.1, and 1.55 Å, respectively. Overall, the structure of GluR3 (flip) S1S2 is very similar to GluR2 (flop) S1S2 (backbone RMSD of 0.30 ± 0.05 for glutamate-bound and 0.26 ± 0.01 for AMPA-bound). The differences in the flip and flop isoforms are subtle and largely arise from one hydrogen bond across the dimer interface and associated water molecules. Comparison of the binding affinity for various agonists and partial agonists suggest that the S1S2 domains of GluR2 and GluR3 show only small differences in affinity, unlike what is found for the intact receptors (with the exception of one ligand, Cl-HIBO, which has a ten-fold difference in affinity for GluR2 vs GluR3).

Keywords

kainate; glutamate receptor; AMPA receptor; willardiine; receptor structure

INTRODUCTION

Ionotropic glutamate receptors (iGluRs) are found on the majority of vertebrate central nervous system neurons and are responsible for the majority of excitatory synaptic transmission.1 In addition to important roles in processes such as learning and memory,2 these receptors have been associated with disorders such as Parkinson's and Alzheimer's diseases, Huntington's chorea, and neurological disorders including epilepsy and ischemic brain damage. iGluRs are composed of four subunits arranged around a central ion channel. Three major subtypes have been identified that are characterized by pharmacological properties, sequence, functionality, and biological role into those that are sensitive: **(1)** to the synthetic agonist N-methyl-D-aspartic acid (NMDA; NR1, NR2A-D, NR3A-B); **(2)** to the synthetic agonist α-amino-3-hydroxy-5-methyl-4-isoxazole-propionic acid (AMPA; GluR1-4); and **(3)** to the naturally occurring neurotoxin kainate (GluR5-7, KA1,2).

Address correspondence to: Robert E. Oswald, Department of Molecular Medicine, Cornell University, Ithaca, NY 14853 USA, Tel. 1-607-253-3877, Fax. 1-607-253-3659, E-Mail: reo1@cornell.edu.

*The authors would like to thank Prof. Eric Gouaux (Vollum Institute) for the GluR2 S1S2J construct and Prof. Linda Nowak (Cornell) for the GluR3 construct. We would also like to thank Melissa D. Thompson and Nabanita De for useful discussions and assistance in handling crystals. This work was supported by a grant from the National Institutes of Health (R01-NS049223). This work is based upon research conducted at the Cornell High Energy Synchrotron Source (CHESS), which is supported by the National Science Foundation under award DMR 0225180, using the Macromolecular Diffraction at CHESS (MacCHESS) facility, which is supported by award RR-01646 from the National Institutes of Health, through its National Center for Research Resources.

The extracellular agonist-binding domain (S1S2 domain) of ionotropic glutamate receptors consists of two lobes with the agonist-binding pocket located between the two lobes.3 The structures of the S1S2 domain from GluR0,4 GluR2,5⁻9 GluR5,10⁻12 GluR6,10،13 NMDA R1,14 and NMDA R215 subtypes have been determined in the presence of a variety of agonists, partial agonists, and antagonists. This has provided structural insights into the processes of channel activation and desensitization as well as the structural basis of the differences in the agonist and antagonist selectivity. In order to understand the physiological role of AMPA receptors and to develop useful therapeutic agents targeted to these widespread receptors, the development of subtype specific agonists and antagonists is of considerable interest.

Although GluR2 and GluR3 are 90.3% identical in the S1S2 agonist-binding domain, several agents have been shown to activate these two subtypes differentially.16⁻19 A mutational analysis suggested that most of the difference in specificity arises from the substitution of a phenylalanine found in GluR3 for a tyrosine in GluR2.20 Although this tyrosine is not found directly in the binding site of GluR2, in some cases, the hydroxyl group can form water-mediated interactions with ligand.21 A homology model of GluR3 has suggested that the loss of these interactions could explain the differences in GluR2 and GluR3 pharmacological properties.18

We describe here the X-ray crystal structure of $GluR3_i$ (flip) S1S2 domain bound to glutamate and AMPA. In addition, a crystal structure of $GluR2_o$ (flop) S1S2 bound to glutamate was obtained with a higher resolution than previously reported.5 The differences between GluR2 and GluR3 are subtle as are the differences in the flip/flop region of the protein (the flip/flop region is an alternatively spliced portion of the protein that can affect desensitization22 and channel closing rate23). Likewise, the binding affinities of agonists and partial agonists to these two binding domains are largely within three-fold, with one exception. The similarities between the two binding domains suggest that the large differences in binding affinity for some ligands may arise only in the intact receptor.

MATERIALS AND METHODS

Materials

Glutamate was obtained from Sigma. AMPA and Cl-HIBO were purchased from Tocris (Ellisville, MO). The willardiine compounds were generously provided by Dr. David Jane (Univ. Bristol) or purchased from Ascent Scientific (Weston-Super-Mare, UK). The GluR2 S1S2J construct was obtained from Eric Gouaux (Vollum Institute).5 The full-length GluR3 flip construct was obtained from Linda Nowak (Cornell University), and the S1S2 domain was produced as described by Armstrong and Gouaux5 for GluR2. The linker region, which replaces the ion channel cassette, consisted of two residues, glycine and threonine.

Protein Preparation and Purification

The $GluR2_o$ and $GluR3_i$ S1S2 proteins were prepared as described by Furukawa and Gouaux14 with slight modification. Briefly, pET-22b(+) plasmids were transformed in *E. coli* strain Origami B (DE3) cells and were grown at 37°C to OD600 of 0.9 to 1.0 in LB medium supplemented with the antibiotics (ampicillin and kanamycin). The cultures were cooled to 20°C for 20 min. and isopropyl-β-D-thiogalactoside (IPTG) was added to a final concentration of 0.5 mM. Cultures were allowed to grow at 20°C for 20 h. The cells were then pelleted and the S1S2 protein purified using a Ni-NTA column, followed by a sizing column (Superose 12, XK 26/100), and finally an HT-SP-ion exchange-Sepharose column (Amersham Pharmacia). Glutamate (1 mM) was maintained in all buffers throughout

purification. After the last column, the protein was concentrated and stored in 20 mM sodium acetate, 1 mM sodium azide, and 10 mM glutamate at pH 5.5.

Radioligand binding

The binding of [^{3}H]AMPA (40 Ci/mmol; Amersham) to GluR2$_o$ and GluR3$_i$ S1S2 was determined as described by Chen *et al.*24 The binding buffer was 30 mM Tris-HCl, 100 mM KSCN, 2.5 mM $CaCl_2$, 10% glycerol, pH 7.2, maintained at all times at 4°C. Glutamate was removed from the S1S2 proteins by successive concentration and dilution as described above, and diluted to a final concentration of 70 nM. After the addition of [^{3}H]AMPA, the reaction (200 μl) proceeded for 1 hour followed by filtration through Millipore GSWP filters and two 2 ml washes with binding buffer. For inhibition assays, [^{3}H]AMPA was used at 10 nM. All analysis was done using Kaleidagraph (Synergy Software).

Crystallization

For crystallization trials, the proteins were concentrated to 0.2 to 0.5 mM using a Centricon 10 centrifugal filter (Millipore, Bedford, MA). AMPA was exchanged into the sample by successive concentration (Amicon Ultra-4 (10K) filter) and dilution using buffer only in the first steps followed by 2 mM (S)-AMPA. The final protein concentration was approximately 0.3 mM. The final ligand concentrations were 10 mM for L-glutamate and 2 mM for (S)-AMPA. All crystals were grown at 4°C using the hanging drop technique, and the drops contained a 1:1 (v/v) ratio of protein solution to reservoir solution. The reservoir solution in case of GluR3-glutamate was 15–16% polyethylene glycol (PEG) 8K, 0.05–0.1 M sodium cacodylate, 0.25 M ammonium sulfate, and 0.1 M zinc acetate (pH 6.5). In case of GluR3-AMPA, the reservoir solution contained 15–17% PEG 1.45K, 0.2 M zinc acetate, and 0.2 M ammonium sulfate, pH 5.0. In case of GluR2-glutamate, the reservoir solution contained 14–17% PEG 8K, 0.1–0.2 M zinc acetate, and 0.1 M sodium cacodylate, pH 6.5.

Construct design

The GluR3$_i$ S1S2 construct was derived from the full-length rat GluR3$_i$ construct provided by Linda Nowak (Cornell). Four primers were used to obtain the S1 and S2 units by PCR and subsequently the S1S2 domain with the GT linker. These primers are **(1)** CAG CGC CAT GGG CAT CAG CAA TGA CAG CTC ACG CGG TGC AAA CCG G **(2)** GCT CTC TAT AGG GGT ACC CTT CTT TAT CAT GAT GGA GAT TCC CAG GC. **(3)** ATG ATA AAG AAG GGT ACC CCT ATA GAG AGC GCT GAA GAC **(4)** GTA CTC GAG TCA GCT GCC GCA CTC TCC TTT GTC GTA CCA C. The PCR products were digested and ligated in the pET-22b(+) vector. Primers 1 and 2 were combined with the full length GluR3 DNA (as template) in one PCR reaction to generate the S1 half of the insert, while primers 3 and 4 were used to synthesize the S2 half. In a third PCR reaction, the S1 and S2 PCR products were used as template with primers 1 and 4 to create the S1S2 insert. The insert was purified, digested and cloned into pET-22b(+) and the authenticity of the construct was confirmed by sequencing both strands. To avoid confusion, full length GluR2 numbering will be used for all comparisons. Supplementary Figure 1 shows the sequence alignment and the sequence numbering for both GluR2 and GluR3 as well as an alternative numbering system that has been used for the isolated S1S2 domains.

Crystal structure determination

Data were collected at the Cornell High Energy Synchrotron Source beam line A1 using a Quantum-210 Area Detector Systems charge-coupled device detector. Data sets were indexed and scaled with HKL-2000.25 Structures were solved with molecular replacement using Phenix.26 Refinement was performed with CNS 1.2,27 and Coot 0.4.1 was used for model building.28

RESULTS

Crystal structure of GluR3 S1S2

The S1S2 domain of GluR3 was produced in a manner identical to GluR2 and expressed as a soluble protein in Origami B. The structures bound to glutamate and to AMPA were solved using molecular replacement with the glutamate-bound S1S2 GluR2 structure (1ftj, A protomer) as a search model. Identical results were obtained with AMPA-bound GluR2 structure (1ftm) used as the search model (Figure 1). The GluR2 S1S2 domain bound to glutamate was crystallized and solved in a similar manner as a control. The glutamate- and AMPA-bound GluR3 structures consist of one copy in the asymmetric unit with a space group of $P222_1$. As described for the previous GluR2 S1S2 glutamate structure,5 three copies were found in the asymmetric unit with a space group of $P2_12_12$. Table 1 gives the data collection statistics.

Table 2 shows the RMSD differences among the GluR2 and GluR3 S1S2 domains bound to glutamate and AMPA. The relative lobe orientations calculated using DynDom29 are not significantly different from the previously reported GluR2 S1S2 structures bound to glutamate (1ftj5). The overall fold of $GluR3_i$ is essentially identical to that of $GluR2_o$. The differences between the domains would therefore arise from subtle differences in the backbone or sidechain conformations or in dynamics. At least on the level of the B factors, little difference was observed between $GluR2_o$ and $GluR3_i$ in either the AMPA- or glutamate-bound forms. Considered below are the differences arising from sidechains and one difference in backbone orientation.

Binding site residues—As shown in Figure 2A & B, GluR2 and GluR3 do not differ in the major contacts with agonists. The one difference that has been discussed in previous studies18,20 is the substitution of Y702 (GluR2) for F702 (GluR3). As shown in Figures 2A and B, the hydroxyl group of the tyrosine changes the configuration of water around the aromatic group in the AMPA-bound form but not in the glutamate-bound form. One fewer water molecule is associated with F702 in $GluR3_i$ relative to the same position in $GluR2_o$ in the AMPA-bound form. This difference presumably arises due to the larger size of AMPA and its proximity to F702. However, glutamate and AMPA do not interact directly with Y/F702, and the loss of the hydroxyl group does not seem to have any direct effect on the configuration of the binding site.

M708 forms part of the binding pocket and changes rotameric states depending upon the size of the ligand (Figures 2C and 2D). Although only one rotameric state was shown in a previous structure of GluR2 S1S2, the higher resolution structure provided here shows two clearly defined states. In one state, the sulfur is oriented toward and is probably hydrogen bonded to the sidechain of T686 as described in the previous reported crystal structure (1ftj). In the alternative state, the sulfur is oriented toward, and makes hydrogen bonds to, the sidechain hydroxyls of T707 and Y732. The orientation of the corresponding sidechain in GluR3 (M708) is the same as the alternative conformation in GluR2. Because of a potential steric clash with the isoxazole ring of AMPA, M708 is rotated away from the binding site in both GluR2 and GluR3, with only a small difference in the orientation of the methyl group between the two subtypes. The multiple orientations of M708 in the glutamate-bound structure are consistent with more dynamics in the glutamate- vs. AMPA-bound form.30,31

Multiple conformations of the D651-S652 peptide bond—The original glutamate-bound structures (1ftj) exhibit two orientations of the trans peptide bond between D651 and S652 in Lobe 2.5 In one protomer, the carbonyl of S652 forms a hydrogen bond with the amide of G451 (Lobe 1) and the carbonyl of D651 forms a water-mediated hydrogen bond network with the amide of Y450 (Figure 2E). In another, the peptide bond is flipped by 180°

and these hydrogen bonds are not present. A third conformation is poorly defined. In all protomers of the AMPA-bound GluR2 structure (1ftm5), the hydrogen bonds are formed. The conformation of the D651-S652 peptide bond is compatible with the formation of these hydrogen bonds in all three protomers reported here for the glutamate-bound $GluR2_o$ S1S2 form as well as in the glutamate-and AMPA-bound forms of $GluR3_i$ S1S2. The AMPA-bound structure is essentially identical to the corresponding GluR2 structures. Although the peptide bond is in the conformation permissible to form the hydrogen bonds, the distance between the carbonyl oxygen of S652 and the amide nitrogen of G451 of glutamate-bound $GluR3_i$ is more than 4 Å, suggesting a weak or nonexistent hydrogen bond.

Dimer interface—The flip and flop forms of $GluR2_o$ and $GluR3_i$ differ in the rates of desensitization22 and sensitivity to regulators of desensitization.32 Although the flip/flop cassette extends beyond the boundary of the S1S2 domain, four residues that differ between flip and flop lie within S1S2 (T744, P745, S754, V758 for flip and N744, A745, N754, L758 for flop; Figure 3A). The intact receptor is thought to be constructed from dimers of dimers, and the interface between S1S2 dimers is near the flip/flop residues.33 Thus, the structure of the dimer interface is of interest. Although only one unique copy is observed, a dimer interface similar to that observed for GluR2 can be observed from the crystal packing. The largest difference in flip and flop is the sensitivity to cyclothiazide, a compound that blocks desensitization32 and stabilizes the dimer interface.33 The $GluR2_o$ S1S2 domain can bind cyclothiazide with only the N754S mutation.33 However, in the absence of cyclothiazide, desensitization is four-fold faster in the flop than the flip form.22 In addition, the rate of channel closing is four-fold faster in the $GluR3_o$ (flop) form than in the corresponding flip form.23 At the S754/N754 position, the backbone of GluR3 flip is identical to both GluR2 flop (1ftj)5 and flip (1uxa)34. The sidechains of N754 and S754 both form a hydrogen bond across the dimer interface to the carbonyl of S729 (Figure 3B). However, the shorter length of the Ser sidechain provides a larger cavity that is filled by an ordered array of water. GluR2(flip; 1uxa) exhibits a similar ordered array of water. The serine hydroxyl can then make multiple water-mediated hydrogen bonds to S729. In the case of the flop isoform, the NH_2 group can make a hydrogen bond directly to S729, but the prevalence35 of hydrogen bonds of Asn sidechains to carbonyls is much lower than that of Ser sidechains. Also, the water matrix is not clearly ordered as it is in GluR3(flip)-glutamate. In the case of the GluR3(flip)-AMPA structure, two waters are in position to make additional water-mediated hydrogen bonds between S754 and S729.

Comparison of GluR2 and GluR3 S1S2 binding affinity

The similarity between the structures of GluR2 and GluR3 S1S2 domain would suggest that the binding affinity for the isolated domains should show little difference. The binding affinity for [^{3}H]AMPA was measured by direct equilibrium radioligand binding and is shown in Figure 4A. The difference in K_D between the two subtypes was less than two-fold. A series of agonists, partial agonists, and antagonists were then tested for differences in IC_{50} between GluR2 and GluR3 S1S2 for inhibition of [^{3}H]AMPA binding (Figure 4B). This panel included several willardiine derivatives for which large differences in affinity between the two subtypes have been observed in the intact receptor. In most cases, the differences in IC_{50} were less than threefold. The results are consistent with the highly conserved structural similarity between the two subtypes in the binding domain, suggesting that differences in affinity for the full-length receptor may arise from large differences between the subtypes in other parts of the protein. The one exception is Cl-HIBO, which shows a ten-fold difference in affinity between GluR2 and GluR3.

DISCUSSION

The structure of $GluR3_i$ S1S2 domain bound to glutamate or AMPA differs in some details from the corresponding structures of $GluR2_o$, but overall, the similarity is striking. Despite the similarity, a number of subtle but possibly important structural features in the binding site and at the dimer interface can be deduced from the higher resolution structure of $GluR2_o$ S1S2 bound to glutamate and the structures of $GluR3_i$ S1S2 bound to glutamate and AMPA. The binding experiments largely support the similarity between the two binding domains, suggesting that the large differences observed in previous studies16–19 may, at least in some cases, arise from differences in the full-length receptors, with GluR3 S1S2 differing significantly from the intact receptor.

Greenwood *et al.*18 produced a homology model of the binding domain of GluR3 and predicted that the differences in affinity were due to the destabilization of a water molecule that form hydrogen bonds with Y702 and T686 in GluR2 (position 702 is an F in GluR3). In GluR2 S1S2 bound to willardiine and fluorowillardiine, this water molecule also interacts with the 4-position carbonyl oxygen. The affinity of willardiine and fluorowillardiine for $GluR2_o$ expressed in insect cells is 10-fold higher than that for $GluR3_o$18 and the affinity of homomeric GluR216 for Cl-HIBO is approximately 100-fold greater than GluR3 in the same expression system. The difference in this water molecule was proposed as the reason for the difference in affinity.18 The crystal structure of GluR2 and GluR2-Y702F shows some differences in the binding of Br-HIBO.7 The Y702F mutation results in a change of the rotameric state of L650 and destabilizes the water network hydrogen bonded to the isoxazole hydroxyl group, resulting in the addition of a long hydrogen bond to the NH of G705 and presumably leading to the difference in affinity for wildtype vs. Y702F. Similarly, Banke *et al.*20 found that mutating the corresponding position in GluR1 from Y to F decreased affinity for Br-HIBO to a value similar to GluR3, and mutating GluR3 from F to Y increased affinity for Br-HIBO although not to the level of GluR1. When bound to glutamate, the water molecules in the binding pocket of GluR3 are identical to those in GluR2 (Figure 2A). However, in the presence of AMPA, one water molecule is lost in GluR3 relative to GluR2. This water hydrogen bonds to the hydroxyls of Y702 and T686; however, does not appear to lead to a substantial stabilization of the binding of AMPA.

The question is whether addition or subtraction of the hydroxyl group of Y702 and a possible change in the corresponding water molecule can change affinity by 10-fold or more for some ligands. The difference in affinity for UBP277 and fluorowillardiine binding to GluR2 S1S2 *vs.* GluR3 S1S2 is less than 2-fold and less than 3-fold for willardiine. The antagonist UBP277 was tested because the 3-carboxylethyl group had the potential to provide more selectivity. Although a direct comparison of the results with the intact homomeric receptors with the isolated binding domains suffers from differences in conditions and possible cooperativity, the results obtained here with both GluR2 and GluR3 S1S2 were more similar to previous studies with heterologously expressed homomeric GluR2 than to GluR3.16,18,20,36 Thus, it appears that while the previously predicted change in hydration of the binding site can occur, the effect on binding affinity is not observed in the isolated domain for the willardiine derivatives and suggests that more than just the binding domain may be involved in the differences in affinity between GluR2 and GluR3. The exception is Cl-HIBO, which does show a significant difference in affinity between GluR2 and GluR3, although less than that of the Y702F mutant of GluR2.7,16

Several details of the binding site in both GluR2 and GluR3 are consistent with previous reports that the glutamate-bound structure may be more dynamic than the AMPA-bound structure.30,31 M708 (GluR2 numbering) is associated with the G subsite of the agonist-binding site5 and changes rotameric states dependent upon the size of the bound agonist.

When glutamate is in the binding site, it adopts an extended conformation, but in the AMPA-bound state a 60° change in the χ^2 torsion angle moves the methyl and sulfur atoms to make room for the larger isoxazole ring of AMPA. The glutamate-bound GluR2 structures reported here clearly show two conformations (differing by 180° in the χ^2 angle) for M708, both in the extended form (Figure 2D). Both conformers form hydrogen bonds, one to the sidechain hydroxyls of T707 and Y732 and the other to the sidechain hydroxyl of T686. The former conformation is that observed in the GluR3 structure (Figure 2C) and the latter was reported previously for GluR2 (1ftj). Although the multiple rotameric states would seem to have little influence on the binding of ligand, it does support previous findings that the agonist binding site is more dynamic in the glutamate-bound form than in the AMPA-bound form,30,31 and further that the lobe 2 side of the binding site is more mobile than the lobe 1 side.37

The D651-S652 peptide bond is another portion of the interface between lobes that can assume multiple conformations. In contrast to the previously reported GluR2 structure (1ftj), the structures determined here all make the two hydrogen bonds across the lobe interface (the search model for molecular replacement was the protomer of 1ftj that does not exhibit the hydrogen bonds). The fact that all three protomers are in this conformation may indicate that this is the predominant form in solution. This conclusion is supported by measurements of residual dipolar coupling by NMR spectroscopy,38 which suggest that this form comprises approximately 90% of the solution conformers for glutamate-bound GluR2 S1S2. This form is stabilized by two hydrogen bonds: one between the carbonyl of S652 and the amide of G451 and the other mediated by a water molecule between the carbonyl of D651 and the amide of Y450 (Figure 2E). The $GluR3_i$ structure is also in this conformation; however, the distance between the carbonyl oxygen of S652 and the amide nitrogen of G451 is greater than 4 Å, suggesting that the hydrogen bond, if present, would be weak. Even with $GluR2_o$ S1S2, substantial differences in the stability of the S652-G451 and the D651-Y450 hydrogen bonds are observed in hydrogen-deuterium exchange experiments (Fenwick and Oswald, unpublished observations), with the S652-G451 hydrogen bond appearing to be considerably weaker.

The backbone conformation at the dimer interface is essentially identical for flip ($GluR2_i$ [1uxa34] and $GluR3_i$) and flop ($GluR2_o$) forms. The RMSD for helices J and K between $GluR3_i$ and $GluR2_o$ is 0.18 ± 0.03 and between $GluR2_i$34 and $GluR3_i$ is 0.19 ± 0.02 (glutamate-bound forms). The flip and flop forms of AMPA receptors arise from alternative splicing39 and show differences in desensitization rates, with flop desensitizing approximately 4-fold faster than flip22 and exhibiting a 4-fold faster rate of channel closing. 23 In addition, the flip, but not the flop, form can bind cyclothiazide, which effectively blocks desensitization. The binding of cyclothiazide stabilizes the dimer interface, suggesting that it is the separation of this interface that contributes to the process of desensitization.33 Of the four positions that differ between the flip and flop forms, N754 (flop)/S754 (flip) makes the only contact across the dimer interface. Also, the N754S mutation confers cyclothiazide sensitivity to the flop form. In the $GluR2_o$ (flop) form, the sidechain of N754 hydrogen bonds to the backbone carbonyl of S729 across the interface. In the $GluR3_i$ (flip) and GluR2i (flip)34 forms, the backbone is in approximately the same position, so that the hydroxyl of S754 is further from S729 than in the flop form. Nevertheless, a water-mediated hydrogen bond can form, and in fact, more than one water is in position to make the hydrogen bond. The high frequency of sidechain hydrogen bonds for serine residues seems to be at least partially due to the ability to rotate the hydroxyl proton into the correct position for the bond.35 Although it cannot be measured directly from the structures, the difference in phenotype between flip and flop may be due to the relative stability of this hydrogen bond, with the water-mediated serine hydrogen bond stabilizing the dimer interface to a somewhat greater extent than the corresponding Asn hydrogen bond.

CONCLUSION

The structure of the flip form of GluR3 bound to glutamate and AMPA is reported here in addition to a higher resolution structure of the flop form of GluR2 bound to glutamate. The structures are very similar but the details provide new information on the differences between subtypes and the nature of the agonist-binding site. The change from Y to F in the 702 position can change, in some cases, the degree of hydration of the binding site, but this does not lead to a drastic change in binding affinity. Using a battery of glutamatergic ligands, only small differences in binding affinity were observed between the S1S2 domains of GluR2 and GluR3. The affinities for GluR2 were similar to that observed in the intact receptor; whereas, the binding to the S1S2 domain of GluR3, in some cases, was of much higher affinity, suggesting that regions outside of the binding domain contribute to binding affinity at least for this subtype. The exception was Cl-HIBO, which shows a significant difference in affinity between GluR2 and GluR3. The new structures of GluR2 provide more information on multiple conformations of a methionine residue in the binding site and on the dynamics of the D651-S652 peptide bond near the binding site. Given the potential importance of these receptors as therapeutic targets, a better understanding of the binding site as well as the importance of other parts of the protein in determining the binding affinity is essential.

Supplementary Material

Refer to Web version on PubMed Central for supplementary material.

The abbreviations used are

AMPA	α-amino-3-hydroxy-5-methyl-4-isoxazole-propionic acid
iGluR	ionotropic glutamate receptor
Br-HIBO	4-bromohomoibotenic acid
Cl-HIBO	4-chlorohomoibotenic acid
$GluR2_i$	the flip form of GluR2
$GluR2_o$	the flop form of GluR2
$GluR3_o$	the flop form of GluR3
$GluR3_o$	the flop form of GluR3
IPTG	isopropyl-β-D-thiogalactoside
NMDA	N-methyl-D-aspartic acid
S1S2	extracellular ligand-binding domain of GluR2
UBP277	(S)-3-(2-carboxyethyl)willardiine

References

1. Dingledine R, Borges K, Bowie D, Traynelis S. The glutamate receptor ion channels. Pharmacol Rev. 1999; 51:7–61. [PubMed: 10049997]
2. Asztely F, Gustafsson B. Ionotropic glutamate receptors. Their possible role in the expression of hippocampal synaptic plasticity. Mol Neurobiol. 1996; 12(1):1–11. [PubMed: 8732537]
3. Oswald RE. Ionotropic glutamate receptor recognition and activation. Advances in Protein Chemistry. 2004; 68:313–349. [PubMed: 15500865]

4. Mayer ML, Olson R, Gouaux E. Mechanisms for ligand binding to GluR0 ion channels: crystal structures of the glutamate and serine complexes and a closed apo state. J Mol Biol. 2001; 311(4): 815–836. [PubMed: 11518533]
5. Armstrong N, Gouaux E. Mechanisms for activation and antagonism of an AMPA-sensitive glutamate receptor: crystal structures of the GluR2 ligand binding core. Neuron. 2000; 28(1):165–181. [PubMed: 11086992]
6. Armstrong N, Sun Y, Chen GQ, Gouaux E. Structure of a glutamate-receptor ligand-binding core in complex with kainate. Nature. 1998; 395:913–917. [PubMed: 9804426]
7. Hogner A, Kastrup J, Jin R, Liljefors T, Mayer M, Egebjerg J, Larsen I, Gouaux E. Structural Basis for AMPA Receptor Activation and Ligand Selectivity: Crystal Structures of Five Agonist Complexes with the GluR2 Ligand-binding Core. J Mol Biol. 2002; 322(1):93–109. [PubMed: 12215417]
8. Jin R, Banke TG, Mayer ML, Traynelis SF, Gouaux E. Structural basis for partial agonist action at ionotropic glutamate receptors. Nat Neurosci. 2003; 6(8):803–810. [PubMed: 12872125]
9. Kasper C, Lunn ML, Liljefors T, Gouaux E, Egebjerg J, Kastrup JS. GluR2 ligand-binding core complexes: importance of the isoxazolol moiety and 5-substituent for the binding mode of AMPA-type agonists. FEBS Lett. 2002; 531(2):173–178. [PubMed: 12417307]
10. Mayer ML. Crystal structures of the GluR5 and GluR6 ligand binding cores: Molecular mechanisms underlying kainate receptor selectivity. Neuron. 2005; 45:539–552. [PubMed: 15721240]
11. Mayer ML, Ghosal A, Dolman NP, Jane DE. Crystal structures of the kainate receptor GluR5 ligand binding core dimer with novel GluR5-selective antagonists. J Neurosci. 2006; 26(11):2852–2861. [PubMed: 16540562]
12. Hald H, Naur P, Pickering DS, Sprogoe D, Madsen U, Timmermann DB, Ahring PK, Liljefors T, Schousboe A, Egebjerg J, Gajhede M, Kastrup JS. Partial agonism and antagonism of the ionotropic glutamate receptor iGLuR5: structures of the ligand-binding core in complex with domoic acid and 2-amino-3-[5-tert-butyl-3-(phosphonomethoxy)-4-isoxazolyl]propionic acid. J Biol Chem. 2007; 282(35):25726–25736. [PubMed: 17581823]
13. Nanao MH, Green T, Stern-Bach Y, Heinemann SF, Choe S. Structure of the kainate receptor subunit GluR6 agonist-binding domain complexed with domoic acid. Proc Natl Acad Sci U S A. 2005; 102(5):1708–1713. [PubMed: 15677325]
14. Furukawa H, Gouaux E. Mechanisms of activation, inhibition and specificity: crystal structures of the NMDA receptor NR1 ligand-binding core. Embo J. 2003; 22(12):2873–2885. [PubMed: 12805203]
15. Furukawa H, Singh SK, Mancusso R, Gouaux E. Subunit arrangement and function in NMDA receptors. Nature. 2005; 438(7065):185–192. [PubMed: 16281028]
16. Bjerrum EJ, Kristensen AS, Pickering DS, Greenwood JR, Nielsen B, Liljefors T, Schousboe A, Brauner-Osborne H, Madsen U. Design, synthesis, and pharmacology of a highly subtype-selective GluR1/2 agonist, (RS)-2-amino-3-(4-chloro-3-hydroxy-5-isoxazolyl)propionic acid (Cl-HIBO). J Med Chem. 2003; 46(11):2246–2249. [PubMed: 12747796]
17. Coquelle T, Christensen JK, Banke TG, Madsen U, Schousboe A, Pickering DS. Agonist discrimination between AMPA receptor subtypes. Neuroreport. 2000; 11(12):2643–2648. [PubMed: 10976936]
18. Greenwood JR, Mewett KN, Allan RD, Martin BO, Pickering DS. 3-hydroxypyridazine 1-oxides as carboxylate bioisosteres: a new series of subtype-selective AMPA receptor agonists. Neuropharmacology. 2006; 51(1):52–59. [PubMed: 16631211]
19. Madsen U, Pickering DS, Nielsen B, Brauner-Osborne H. 4-Alkylated homoibotenic acid (HIBO) analogues: versatile pharmacological agents with diverse selectivity profiles towards metabotropic and ionotropic glutamate receptor subtypes. Neuropharmacology. 2005; 49 (Suppl 1):114–119. [PubMed: 15996690]
20. Banke TG, Greenwood JR, Christensen JK, Liljefors T, Traynelis SF, Schousboe A, Pickering DS. Identification of amino acid residues in GluR1 responsible for ligand binding and desensitization. J Neurosci. 2001; 21(9):3052–3062. [PubMed: 11312290]

21. Jin R, Gouaux E. Probing the function, conformational plasticity, and dimer-dimer contacts of the GluR2 ligand-binding core: Studies of 5-substituted willardiines and GluR2 S1S2 in the crystal. Biochemistry. 2003; 42(18):5201–5213. [PubMed: 12731861]
22. Mosbacher J, Schoepfer R, Monyer H, Burnashev N, Seeburg PH, Ruppersberg JP. A molecular determinant for submillisecond desensitization in glutamate receptors. Science. 1994; 266(5187): 1059–1062. [PubMed: 7973663]
23. Pei W, Huang Z, Niu L. GluR3 flip and flop: differences in channel opening kinetics. Biochemistry. 2007; 46(7):2027–2036. [PubMed: 17256974]
24. Chen GQ, Gouaux E. Overexpression of a glutamate receptor (GluR2) ligand binding domain in Escherichia coli: application of a novel protein folding screen. Proc Natl Acad Sci U S A. 1997; 94(25):13431–13436. [PubMed: 9391042]
25. Otwinowski, Z.; Minor, W. Processing of X-ray diffraction data collected in oscillation mode. In: Carter, CW.; Sweet, RM., editors. Methods in Enzymology, Vol 276, Macromolecular Crystallography, part A. Vol. 276. New York: Academic Press; 1997. p. 307-326.
26. Adams PD, Grosse-Kunstleve RW, Hung LW, Ioerger TR, McCoy AJ, Moriarty NW, Read RJ, Sacchettini JC, Sauter NK, Terwilliger TC. PHENIX: building new software for automated crystallographic structure determination. Acta Crystallogr D Biol Crystallogr. 2002; 58(Pt 11): 1948–1954. [PubMed: 12393927]
27. Brunger AT. Version 1.2 of the Crystallography and NMR system. Nature protocols. 2007; 2(11): 2728–2733.
28. Emsley P, Cowtan K. Coot: model-building tools for molecular graphics. Acta Crystallogr D Biol Crystallogr. 2004; 60(Pt 12 Pt 1):2126–2132. [PubMed: 15572765]
29. Hayward S, Lee RA. Improvements in the analysis of domain motions in proteins from conformational change: DynDom version 1.50. J Mol Graph Model. 2002; 21(3):181–183. [PubMed: 12463636]
30. Ahmed AH, Loh AP, Jane DE, Oswald RE. Dynamics of the S1S2 glutamate binding domain of GluR2 measured using 19F NMR spectroscopy. J Biol Chem. 2007; 282(17):12773–12784. [PubMed: 17337449]
31. Valentine ER, Palmer AG 3rd. Microsecond-to-millisecond conformational dynamics demarcate the GluR2 glutamate receptor bound to agonists glutamate, quisqualate, and AMPA. Biochemistry. 2005; 44(9):3410–3417. [PubMed: 15736951]
32. Partin KM, Fleck MW, Mayer ML. AMPA receptor flip/flop mutants affecting deactivation, desensitization, and modulation by cyclothiazide, aniracetam, and thiocyanate. J Neurosci. 1996; 16(21):6634–6647. [PubMed: 8824304]
33. Sun Y, Olson R, Horning M, Armstrong N, Mayer M, Gouaux E. Mechanism of glutamate receptor desensitization. Nature. 2002; 417(6886):245–253. [PubMed: 12015593]
34. Greger IH, Akamine P, Khatri L, Ziff EB. Developmentally regulated, combinatorial RNA processing modulates AMPA receptor biogenesis. Neuron. 2006; 51(1):85–97. [PubMed: 16815334]
35. McDonald I, Thornton JM. Atlas of side-chain and main-chain hydrogen bonding. 1994
36. Jane DE, Hoo K, Kamboj R, Deverill M, Bleakman D, Mandelzys A. Synthesis of willardiine and 6-azawillardiine analogs: pharmacological characterization on cloned homomeric human AMPA and kainate receptor subtypes. J Med Chem. 1997; 40(22):3645–3650. [PubMed: 9357531]
37. McFeeters RL, Oswald RE. Structural mobility of the extracellular ligand-binding core of an ionotropic glutamate receptor. Analysis of NMR relaxation dynamics. Biochemistry. 2002; 41:10472–10481. [PubMed: 12173934]
38. Maltsev AS, Ahmed AH, Jane DE, Oswald RE. Mechanism of partial agonism at the GluR2 AMPA receptor: Measurements of lobe orientation in solution. Biochemistry. 2008 in press.
39. Sommer B, Keinänen K, Verdoorn TA, Wisden W, Burnashev N, Herb A, Köhler M, Takagi T, Sakmann G, Seeburg PH. Flip and flop: A cell-specific functional switch in glutamate-operated channels of the CNS. Science. 1990; 249:1580–1584. [PubMed: 1699275]

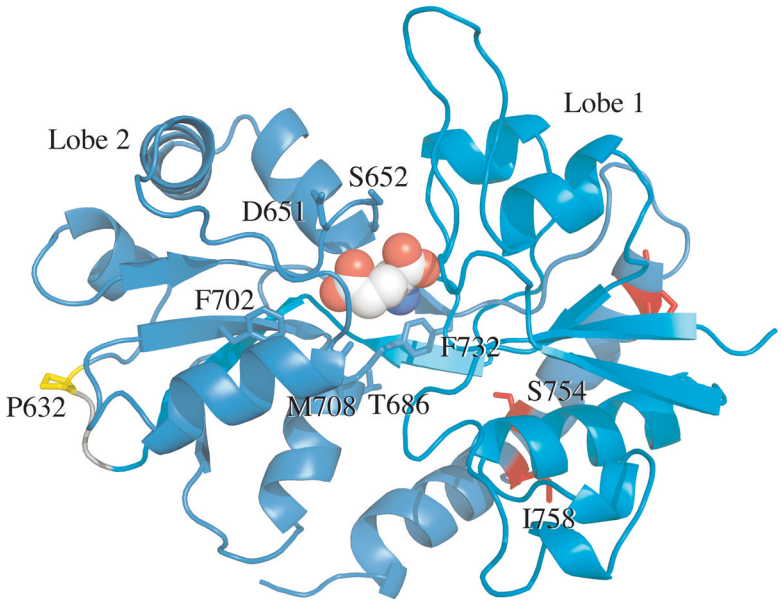

Figure 1.
Structure of GluR3$_i$ S1S2 domain bound to glutamate with a number of residues discussed in the text shown. The S1 sequence is shown in cyan and the S2 sequence in blue. The four residues that differ between flip and flop forms are colored red.

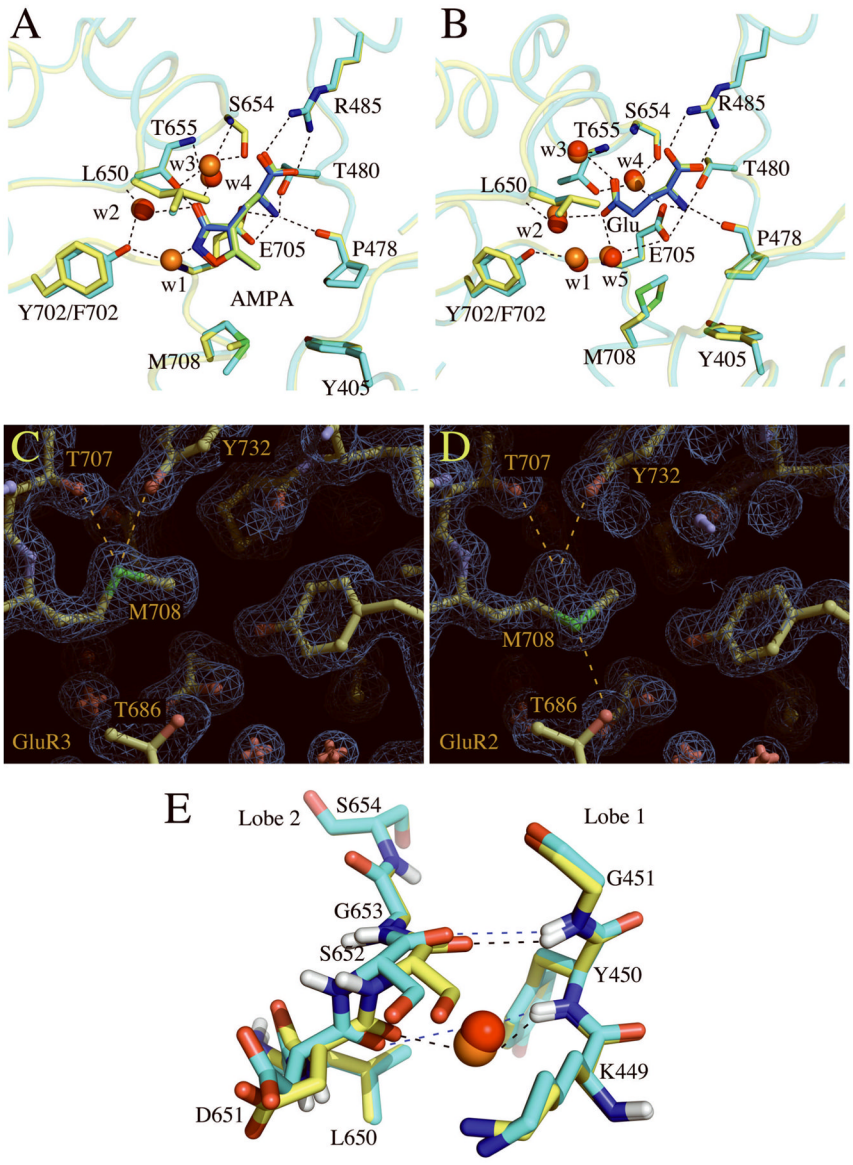

Figure 2.

Binding sites for (A) AMPA bound to $GluR2_o$ (1ftm; cyan) and $GluR3_i$ (yellow) and (B) glutamate bound to $GluR2_o$ (cyan) and $GluR3_i$ (yellow). Water residues in the $GluR2_o$ structures are shown in orange and those in the $GluR3_i$ structures are shown in red. Electron density maps for $GluR3_i$ (C) and $GluR2_o$ (D) bound to glutamate. The alternative conformations of M708 are illustrated for $GluR2_o$. (E) The regions of $GluR2_o$ (cyan) and $GluR3_i$ (yellow) undergoing a rotation of the peptide backbone are illustrated. The S652/G451 hydrogen bond is longer in $GluR3_i$.

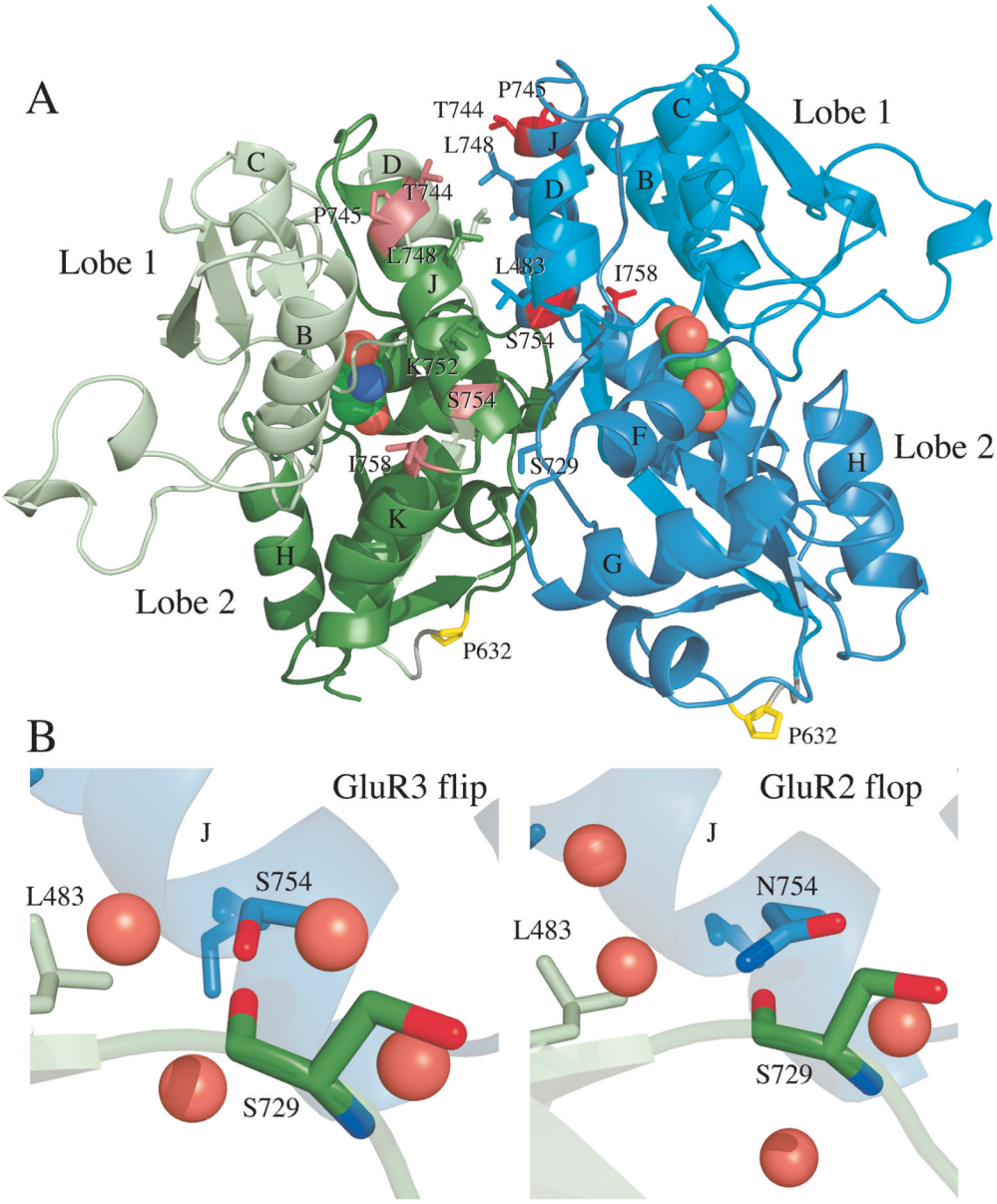

Figure 3.

(A) The dimeric structure of GluR3 bound to glutamate. The helices are labeled as in Armstrong et al.6. Residues participating in contacts across the dimer interface are labeled. P632 (yellow) flanks the artificial linker region of the construct and is the point that connects to the linkers to the ion channel. The four residues that differ in flip and flop are shown in shades of red. (B) The dimer interface at the S754 (flip)/N754 (flop) interaction with S729. Both can form hydrogen bonds, but the structure of the water surrounding the hydrogen bond differs.

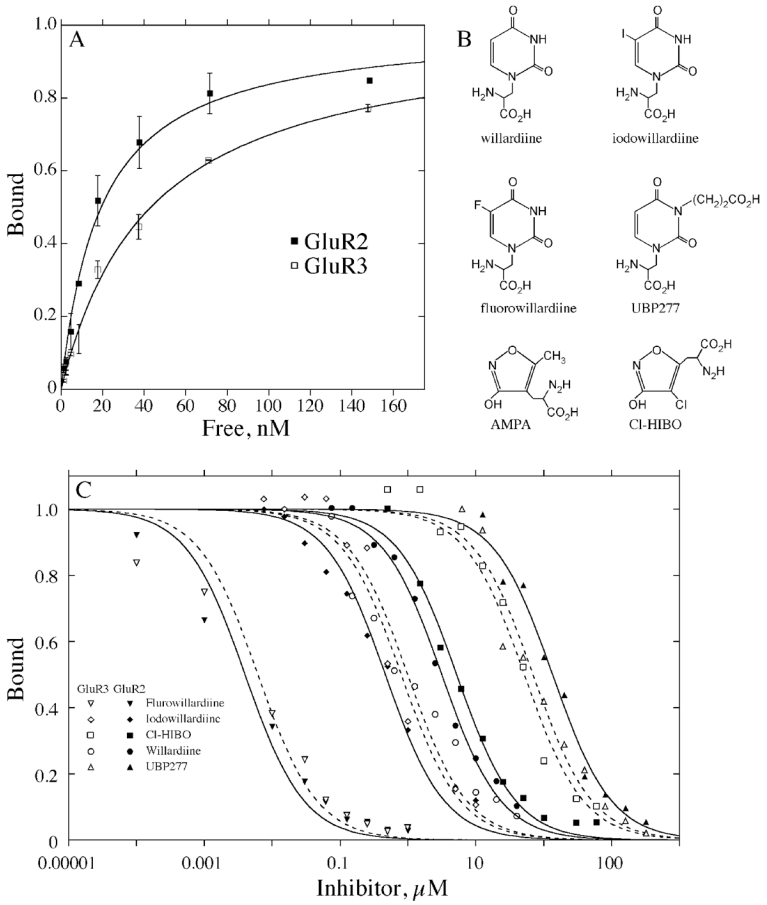

Figure 4.

(A) Binding of [^{3}H]AMPA to the S1S2 domains of GluR2$_o$ and GluR3$_i$. The K_D of binding differed by less than 2-fold: 19 ± 2 nM for GluR2 and 43 ± 5 nM for GluR3. Armstrong and Gouaux5 reported a K_D of 24.8 ± 1.8 nM for [^{3}H]AMPA binding to GluR2. (B) Structures of the ligands used in the binding studies, (C) The inhibition of [^{3}H]AMPA binding by agonists, partial agonists, and antagonist to the S1S2 domains of GluR2$_o$ and GluR3$_i$. Except for willardiine, the IC_{50} values were within 2-fold for the two subtypes: (ligand, GluR2 IC_{50}/GluR3 IC_{50}; IC_{50} expressed in μM) fluorowillardiine, 0.0040±.0009/0.0062±0.0014; iodowillardiine, 0.46±0.05/0.79±0.14; Cl-HIBO, 5.0±0.3/55±4; willardiine, 3.1±0.2/0.99±0.18; UBP277, 135±12/69±10. In all cases, GluR2$_o$ is shown with filled symbols, and GluR3$_i$ is shown with open symbols.

Table 1

Structural Statistics

Structure	**GluR3-glutamate**	**GluR3-AMPA**	**GluR2-glutamate**
Space Group	$P222_1$	$P222_1$	$P2_12_12$
Unit Cell (Å)	a=47.5 b=47.4 c=137.9	a=47.3 b=47.3 c=138.3	a=113.8 b=163.2 c=47.3
X-ray source	CHESS (A1)	CHESS (A1)	CHESS (A1)
Wavelength (Å)	0.977	0.977	0.977
Resolution (Å)	50-1.9 (1.97-1.90)	50-2.1 (2.18-2.10)	50.0-1.55 (1.61-1.55)
Measured reflections (#)	185963	99926	533686
Unique reflections (#)	24081	18629	126527
Data redundancy	7.5 (6.3)	5.4 (5.4)	4.2 (2.4)
Completeness (%)	99.6 (97.8)	99.7 (100.0)	98.2 (83.7)
R_{sym} (%)	13.3 (84.4)	8.2 (33.1)	10.2 (46.2)
I/σ_i	22.2 (5.0)	24.1 (6.7)	13.0 (2.0)
PDB ID	3DLN	3DP4	3DP6
Current Model Refinement Statistics			
Phasing	MR	MR	MR
Molecules/AU	1	1	3 (no NCS applied)
R_{work}/R_{free} (%)	19.7/23.9	21.2/25.8	22.2/24.4
Free R test set size (#/%)	2380 (9.5)	1758 (9.4)	11864 (9.3)
Number of protein atoms	2031	2031	6054
Number of heteroatoms	10	13	30
Rmsd bond length (Å)	.0048	.0053	.0051
Rmsd bond angles (°)	1.2	1.2	1.2
Rmsd B factors ($Å^2$, main/side)	1.26/2.17	1.42/2.47	1.13/1.99

Table 2

RMSD for all heavy atoms

Structure	GluR3 glu	GluR3 AMPA	GluR2 A	GluR2B	GluR2 C
GluR3 glu	-	.271	.244	.328	.312
GluR3 AMPA		-	.323	.306	.300
GluR2 glu A			-	.244	.230
GluR2 glu B				-	.117
GluR2 glu C					-